

Research Article

Cytosine methylation by DNMT2 facilitates stability and survival of HIV-1 RNA in the host cell during infection

Rachana Roshan Dev^{1,2}, Rakesh Ganji³, Satya Prakash Singh⁴, Sundarasamy Mahalingam⁴, Sharmistha Banerjee³ and Sanjeev Khosla¹

¹Centre for DNA Fingerprinting and Diagnostics (CDFD), Hyderabad 500001, India; ²Graduate Studies, Manipal University, Manipal 576104, India; ³Department of Biochemistry, School of Life Sciences, University of Hyderabad, Hyderabad, Telangana, India; and ⁴Laboratory of Molecular Virology and Cell Biology, Department of Biotechnology, Bhupat and Jyoti Mehta School of Biosciences, Indian Institute of Technology Madras, Chennai 600036, India

Correspondence: Sanjeev Khosla (sanjuk@cdfd.org.in)

The enigmatic methyltransferase, DNMT2 (DNA methyltransferase 2), structurally resembles a DNA methyltransferase, but has been shown to be a tRNA methyltransferase targeting cytosine within a specific CpG in different tRNA molecules. We had previously shown that, during environmental stress conditions, DNMT2 is re-localized from the nucleus to the cytoplasmic stress granules (SGs) and is associated with RNA-processing proteins. In the present study, we show that DNMT2 binds and methylates various mRNA species in a sequence-independent manner and gets re-localized to SGs in a phosphorylation-dependent manner. Importantly, our results indicate that HIV-1 enhances its survivability in the host cell by utilizing this RNA methylation capability of DNMT2 to increase the stability of its own genome. Upon infection, DNMT2 re-localizes from the nucleus to the SGs and methylates HIV-1 RNA. This DNMT2-dependent methylation provided post-transcriptional stability to the HIV-1 RNA. Furthermore, DNMT2 overexpression increased the HIV-1 viral titre. This would suggest that HIV hijacks the RNA-processing machinery within the SGs to ensure its own survival in the host cell. Thus, our findings provide for a novel mechanism by which virus tries to modulate the host cell machinery to its own advantage.

Introduction

Stress granules (SGs) are dynamic, non-membranous cytoplasmic RNA–protein aggregates formed in response to a variety of environmental stresses and as a consequence of reduced or abortive translation machinery in the cell [1,2]. They serve as a reservoir of translationally silent mRNA, whose fate is conditional upon release from the SGs once the stress condition is alleviated [2,3]. The repertoire of proteins common to most of the SGs includes modulators of RNA processing including splicing, RNA transport, RNA stability and translation [4–9]. However, the complete list of proteins that reside in SGs varies depending on the cue of stress. In addition, proteins that are not normally associated with RNA processing like HDAC6, DNMT2 (DNA methyltransferase 2), epithelial cell transforming 2, Aurora kinase B and TRAF-2 have also been found to be residing within the SGs [10–13].

DNMT2, a DNA methyltransferase based on its structure, shows very residual catalytic activity for DNA and has been shown to methylate tRNA molecules especially cytosine at position 38 of Asp, Gly and Val tRNA [14–16]. A highly conserved protein, DNMT2, is the only known enzyme which uses a DNA methyltransferase-like catalytic mechanism to methylate tRNA [17]. Even though the knockout of *Dnmt2* failed to show any significant phenotype in mice and *Drosophila*, the protein has been found to play a role in cell physiology in a wide range of organisms. In Zebrafish, morpholino knock-down of *Dnmt2* caused organ differentiation defects [18]. In *Drosophila*, *Dnmt2* has

Received: 6 April 2017
 Revised: 2 May 2017
 Accepted: 4 May 2017

Accepted Manuscript online:
 5 May 2017
 Version of Record published:
 6 June 2017

Dicer-2-dependent siRNA pathway activity and provides genomic stability and longevity [19–21]. In mice, it is required for protein synthesis and fidelity, and is associated with RNA-mediated epigenetic inheritance [22,23]. Various studies have pointed to the role of Dnmt2 as a part of cellular response to various environmental stresses. In *Physcomitrella patens*, Dnmt2 helps in recovery from osmotic and salt stress [24]. In *Drosophila*, Dnmt2-mediated methylation protects tRNA from stress-induced cleavage [15]. Previous work from our laboratory had elucidated the role of DNMT2 in RNA processing during cellular stress in mammalian cells. DNMT2, a protein that localizes predominantly in the nucleus, re-localized to SGs in the cytoplasm in response to environmental stress and interacted with several proteins involved in RNA processing [11].

However, the reason for the presence of DNMT2 in SGs has remained an enigma. What could be the role of a DNA/tRNA methyltransferase in the SGs, an abode predominantly enriched in untranslated mRNA molecules? Moreover, in our previous study, we had also reported misregulation of several genes involved in host response to viral infection. Since viral infections are known to be correlated with nucleation of SGs, could this suggest involvement of DNMT2 in the mechanism of host cell response to viral infection? In the present study, we show that similar to what happens during various environmental stress conditions, infection of mammalian cells by HIV-1 also causes dynamic re-localization of DNMT2 from the nucleus to cytoplasmic SGs. Importantly, we show that DNMT2 can bind to and methylate HIV-1 RNA. But this RNA binding and methylation capability of DNMT2 were not limited to HIV-1 RNA. DNMT2 was able to bind and methylate cellular mRNA molecules in a sequence-independent manner. Interestingly, HIV-1 titre increased with overexpression of DNMT2. In light of our finding that DNMT2 improves the stability of HIV-1 RNA, we believe that HIV-1 could be utilizing this RNA methylation capability of DNMT2 to increase the stability of its own genome and enhance its survivability in the host cell.

Materials and methods

Cloning, expression and purification of DNMT2

DNMT2 was PCR-amplified from cDNA generated from HEK293 cells with the following gene-specific primers

DNMT2 EcoRIFP-5'-GAAGAATTCATGGAGCCCCCTGCGG-3'
DNMT2 BamH1FP-5'-GGAGGATCCATGGAGCCCCCTGCGG-3'
DNMT2 ApairP-5'-GGGGGGCCCTTATTCATATAAGATTTGATTAGTTAG-3'
DNMT2 EcoRIRP-5'-GAAGAATTCTTATTCATATAAGATTTGATTAGTTAG-3'

and cloned into mammalian expression vector pcDNA-EGFPMCS at the *EcoRI*-*ApaI* sites and in pcDNA-SFB vector in *BamHI*-*ApaI* sites. DNMT2 was also cloned into bacterial expression vector pET28a+ in *BamH1*-*EcoR1* sites containing the N-terminal 6×His tag. 6×His-DNMT2 was overexpressed in *E. coli* BL21-DE3 cells using 0.2 mM IPTG at 18°C overnight. Protein purification was done in Tris-Cl buffer following the established protocol [25].

Transient transfections and infections

Vector alone or GFP or SFB (Protein S-Flag-Biotin)-tagged DNMT2 (WT or phospho-mutants) was transfected into HEK293 cells [a kind gift from Dr Gayatri Ramakrishna, who obtained it from the Cell Culture Stock Centre at National Centre for Cell Science (NCCS), Pune] using Lipofectamine 2000 as per the manufacturer's protocol (Invitrogen).

For siRNA-based DNMT2 repression, HEK293 cells were transfected with DNMT2 siRNA (GE Dharmacaon, On-TARGET plus) using Lipofectamine RNAiMAX (Invitrogen) reagent in OptiMEM as per the manufacturer's protocol.

Infections with HIV-1 were done either in CEMx174 or SupT1 cells. CEMx174 cells (2×10^6) were infected with 20 ng of freshly purified virus per well (titrated by the p24 assay) in the presence of 2 µg/ml polybrene in RPMI 1640. After removal of the residual virus, cells were seeded again in RPMI complete media. SupT1 cells were infected by adding 30 ng/ml of p24 equivalent virus in serum-free RPMI. Media were changed to complete RPMI with 10% FBS after 2 h of infection. Cells were harvested at defined time points. For mock infections, HIV-1 particles were heat-inactivated for 30 min at 70°C. The infections were performed in the BSL-II type-II negative pressure facility of either Dr S. Mahalingam, IIT Madras, Chennai or Dr Sharmistha Banerjee

in the University of Hyderabad, Hyderabad after taking appropriate Institutional Biosafety Committee approval.

Osmotic, oxidative and pH stress

For osmotic and oxidative stress, HEK293 cells were treated with 0.5 M sorbitol for 30 min (osmotic stress) or 0.5 mM sodium arsenite for 1 h (oxidative stress). For pH stress, HEK293 cells were incubated in HBSS buffer (pH 5.7) (Hank's buffer — 0.137 M NaCl, 5.4 mM KCl, 0.25 mM Na₂HPO₄, 0.1 g glucose, 0.44 mM KH₂PO₄, 1.3 mM CaCl₂, 1.0 mM MgSO₄, 4.2 mM NaHCO₃) for 25 min followed by PBS wash.

Preparation and quantification of infectious HIV-1 particles

HEK293T cells were transfected with pNL4.3 (HIV-1 proviral DNA) with the calcium phosphate method. Culture supernatant was collected 24 h after transfection and filtered through 0.45 µM filter (Millipore), precipitated using polyethylene glycol and quantified by the HIV-1 p24 ELISA kit (Advanced BioScience Laboratories, Inc.) according to the manufacturer's protocol [26].

Immunofluorescence

Cells were washed with PBS, 12, 24 or 48 h post-transient transfection or infection, and fixed in 3.7% formaldehyde followed by cell permeabilization with 0.1% Triton X-100. DNMT2 antibody was used for immunostaining at a 1:200 dilution at 4°C overnight. Anti-rabbit antibody conjugated to Alexa Fluor 488 or 586 (Invitrogen) was used at a 1:2000 dilution for 1 h at room temperature. Cells were mounted using DAPI containing Vectashield (Vector Laboratories) and examined by a confocal microscopy.

RNA pull-down assay and differential display PCR

Total RNA was isolated from untreated HEK293 cells or HEK293 cells treated with 0.5 mM sodium arsenite for 1 h, or HIV-1-infected and uninfected SupT1, using Trizol (Sigma) as per the manufacturer's protocol. A 20 µg aliquot of 6×His-DNMT2 bound to Ni-NTA agarose was incubated with 5 µg of total RNA. RNA pull-down and differential display PCR were performed as mentioned elsewhere [27]. For PCR amplification, primers HT11A (5'-AAGCTTTTTTTTA-3') and arbitrary primer AP3 (5'-AAGCTTGTCAG-3') were used. For reverse transcription, HT11A primer was used. The PCR products were resolved on 6% Urea-PAGE. The amplified bands were excised and eluted from polyacrylamide gel, and the re-amplified bands were cloned into the pBSK-TA vector. Positive clones were sequenced.

In vitro transcription

The cloned RNA sequences were *in vitro*-transcribed using the T7 or T3 promoter present in the pBSK-TA vector. Reaction mixture [1 µg template, 1× reaction buffer, 10 mM UTP, 10 mM ATP, 10 mM GTP, 10 mM CTP and T7 RNA Polymerase (Fermentas), T3 RNA pol (NEB)] was incubated for 1 h at room temperature, followed by DNase treatment for 15 min at 37°C. RNA was extracted by phenol-chloroform, ethanol-precipitated overnight at -80°C and resuspended in RNase-free water. For radioactive *in vitro* transcription, 100 µM cold CTP and 2 µl α³²P-CTP were used. Free nucleotides were removed by the Nucleotide Removal Kit (Qiagen). *In vitro*-transcribed RNA was quantified on a Urea-PAGE.

The following primers were used for cloning the various regions from HIV.

HIV9F-5'-CAGTGGATATAGAACAGAAGTTATTTC-3'
HIV9R-5'-GTCCTTCCAAAGTGGATTCTG-3'
HIV13F-5'-ACCCACAAGAAGTAGTATTGGTAATG-3'
HIV13R-5'-TACATGGCCTGTTCCATTGAACG-3'
HIV18F-5'-AGCACACAAGAGGAGGAGGAGGTG-3'
HIV18R-5'-TCGATGTCAGCAGTTCTGAAGTAC-3'

For HIV-1 RNA the co-ordinates for the various regions analyzed are as follows:

HIV9:4015–4487
HIV13:6009–6488
HIV18:8519–8969

RNA-EMSA

RNA was *in vitro*-transcribed using $\alpha^{32}\text{P}$ -CTP and used as the probe for DNMT2 in RNA-EMSA. The binding reaction was performed at 37°C for 30 min as mentioned elsewhere [28]. The cold competition assay was performed using 10 \times or 100 \times cold competitor [DNA, specific or non-specific RNA and poly (dI-dC)]. For competition assay, cold competitor was incubated with protein for 10 min followed by the addition of the probe.

RNA methyltransferase assay

For the RNA methylation assay, 300 ng of RNA substrate (*in vitro*-transcribed) and 300 ng of purified 6 \times His-DNMT2 were incubated in methylation reaction buffer [10 mM Tris (pH 8.0), 1 mM EDTA, 1 mM DTT, 40 mM NaCl, 400 ng/ml BSA and 10 mM MgCl₂] with 200 μ M SAM for 2 h at 37°C. RNA was purified after proteinase K treatment by the phenol-chloroform method and resuspended in 10 μ l of RNase-free water.

RNA bisulphite sequencing

The RNA incubated with DNMT2 protein in the methyltransferase assay was subjected to bisulphite conversion as described elsewhere [15]. Bisulphite-converted RNA was used as the template for cDNA synthesis. PCR amplification was done using bisulphite-converted RNA-specific primers. The PCR product was cloned into plasmid pBSK-TA vector followed by sequencing. Methylation analysis was done on at least 15–20 clones for each RNA species. Primers used for bisulphite PCR are as follows:

RPL27ABS1F-5'-TAGTTATTTAGGTTATTTGGGAAAG-3'
RPL27ABS1R-5'-TTAACCAAAATTTATAAAAAAAAATAT-3'
HIVBS18bF-5'-TGGAAAGGGTTAATTATTTTAAAG-3'
HIVBS18R-5'-ATATCAACAATTCTTAAAATACTCCG-3'

Filter binding assay

The RNA methylation assay was performed with 2 μ M tritiated S-adenosylmethionine (^3H -SAM) as the methyl group donor. RNA precipitated with 10% TCA was spotted on GF/C filters pre-soaked with 50 μ M cold SAM. Filters were washed with 10% TCA, water and 95% ethanol sequentially. Filters were dried at 70°C and soaked in 4 ml of scintillation fluid, and scintillation counts (DPMs) were taken in the Tri-Carb Scintillation Counter (PerkinElmer).

Methylated RNA immunoprecipitation

HEK293 were transfected with pcDNA-SFB and pcDNA-SFB-DNMT2 followed by sodium arsenite treatment (2.5 mM for 25 min) 24 h post-transfections. Cells were fixed using 1% formaldehyde and quenched with 125 mM glycine. SFB-DNMT2-bound RNA was pulled down from total cell lysate using streptavidin agarose beads and eluted with biotin (2 mg/ml). The eluted RNA was reverse cross-linked at 70°C for 15 min, precipitated after phenol-chloroform extraction, sonicated and subjected to immunoprecipitation with the 5-methyl cytosine antibody (IP star — as per the manufacturer's protocol, Diagenode) that has been also shown to detect 5-methyl cytosines in RNA [30]. The precipitated RNA was subjected to DNase treatment (Invitrogen) followed by cDNA synthesis using random hexamers. Semi-quantitative RT-PCR was performed using RPL27A, BRWD1 and CNNM3-specific primers. pcDNA-SFB-transfected cell lysate was taken as control.

Primers used for MeRIP-RT PCR were as follows:

RPLRT5F-5'-TCGGTGTTTATCCTGGTTC-3'
RPLRT5R-5'-TGGGTGGCTAGGAAGAGGTA-3'
CNM3RT1F-5'-GCCAGGCTGATCTGAACTC-3'
CNM3RT1R-5'-AATTGCCAGGTGATTCTGG-3'
BRWD1RT2F-5'-TCTTGCAGCCATGAACAGTC-3'
BRWD1RT2R-5'-GTCTGGAACTTCAGGCAGG-3'

For performing MeRIP on HIV-1 RNA, HEK293T cells transfected with pcDNA-SFB/pNL4.3 or pcDNA-SFB-DNMT2/pNL4.3 were fixed using 1% formaldehyde. HIV-1 RNA bound to DNMT2 was pulled down with

streptavidin agarose beads (GE) and processed as above. Semi-quantitative RT-PCR was done using the following HIV-1 genomic RNA-specific primers:

HIV18F-5'-AGCACAAAGAGGAGGAGGAGGTG-3'
HIV18R-5'-TCGATGTCAGCAGTTCTGAAGTAC-3'

Fluorescent *in situ* hybridization

HEK cells were seeded in chamber slides at a density of 1×10^5 cells/chamber in DMEM and transfected with pcDNA-EGFP-DNMT2 in OptiMEM medium using lipofectamine as per the manufacturer's instructions (Invitrogen). pcDNA-EGFP MCS-transfected cells were used as control. Cells were fixed using 3.7% formaldehyde 48 h post-transfection, permeabilized in 70% ethanol and incubated overnight at 4°C. After three PBS washes, the cells were incubated for 2 h in hybridization buffer (2× SSC, 100 µg of BSA, 10% Dextran sulphate, 50 µg of yeast total RNA, 50 µg of salmon sperm DNA and 70% formamide) with the mRNA probes (1 nM each) at 50°C as described elsewhere [29]. Fluorescently labelled DNA probes were prepared for RPL27A, BRWD1 and CNNM3 using Chromatide Alexa Fluor 546-14-dUTP (Invitrogen) by PCR as per the manufacturer's protocol (Invitrogen) using the following primers:

RPLFSHF-5'-CTGCCTCTGACATTGTCGGTG-3'
RPLFSHR-5'-GCAGTGACAGTAGGCAGTGCTACG-3'
CNNM3FSHF-5'-CTCAAGGAATAAACTCTGAGAGCAAG-3'
CNNM3FSHR-5'-GAGGTCGAGGCTGCAGCAAG-3'

After hybridization, cells were rinsed with 2× SSC, 0.5% SDS for 5 min, 2× SSC, 10% formamide, 0.5% SDS for 10 min and in 2× SSC, 0.5% SDS for 5 min. Cells were mounted using Vectashield containing DAPI followed by a confocal microscopy.

For HIV-FISH, SupT1 cells were harvested post HIV-1 infections at required time points. Cells were fixed using 3.7% formaldehyde after 48 h of transfections and processed for RNA-FISH as mentioned above. Fluorescent-labelled DNA probes against HIV-1 RNA were PCR-amplified (using primers mentioned earlier in the section on *in vitro* transcription) using cy3- dUTP (in Figure 4, Sigma) or 568-5-dUTP (in Figure 6, Invitrogen) as per the manufacturer's protocol followed by PCR purification.

HIV-1 mRNA stability assay

HEK293 cells were co-transfected with pNL4.3 proviral DNA along with GFP or GFP-DNMT2 in the BSL-II type-II negative pressure facility in the Laboratory of Dr Sharmistha Banerjee in the University of Hyderabad, Hyderabad. Cells were washed with PBS twice and the media were changed with complete DMEM (10% FBS) supplemented with Actinomycin D (5 µg/ml; Sigma) 12 h after transfection to stop cellular transcription. Cells were fixed at different time points and processed for FISH as mentioned above. As a control, to test the effect of Actinomycin D on transcription, total proteins isolated from HEK293 cells cultured as above in the presence of Actinomycin D were western blotted and probed for Cyclin D1. As shown in Supplementary Figure S16, the Cyclin D1 level was significantly reduced in the presence of Actinomycin D.

Quantification of fluorescent *in situ* hybridization for HIV RNA/mRNA stability

Cells were fixed at different time points and processed for RNA-FISH as mentioned above; HIV-1 RNA intensity and RPL27A RNA intensity were quantified for randomly selected fields in cells expressing GFP/pNL4.3 and GFP-DNMT2/pNL4.3 and GFP or GFP-DNMT2-transfected cells. The imaging settings for confocal imaging were kept constant for all the images. The brightness and contrast for all the images were constant for all fields in each sample. The signal intensity was quantified using Image J, and the raw integrated intensity for each GFP-DNMT2-expressing cell was calculated.

HIV-1 RNA stability analysis by real-time PCR

HEK293T co-transfected with pNL4.3 and GFP/GFP-DNMT2 and treated with Actinomycin D (as mentioned above) were harvested 24 and 48 h post-transfections. RNA was isolated using Trizol reagent as per the manufacturer's protocol (Sigma). A 1 µg aliquot of RNA was converted into cDNA using Superscript III

(Invitrogen). The change in expression of HIV-1 mRNA upon overexpression of DNMT2 was evaluated by real-time PCR using Mesa Green qPCR Mastermix Plus (Eurogentec) in the ABI Prism SDS 7500 system. 18s rRNA was used as an internal control. RNA was quantified using the Nanodrop Spectrophotometer. Primers were designed immediately downstream from the 3' poly-A sequence to avoid any reverse transcription bias because of nucleotide methylation of HIV-1 mRNA.

The primers used for real-time PCR were as follows:

SKNEFRTF-5'-AGCTTGTACACCCCTGTGAGC-3'
SKNEFRTR-5'-CTTGAAGTACTCCGGATGCAG-3'
18SrRNAF-5'-GGCCCTGTAATTGGAATGAGTC-3'
18SrRNAR-5'-CCAAGATCCAACTAGCAGCTT-3'

Kinase assay

The kinase domain of ATM kinase was cloned into the pCDNA3.1-SFB vector in the *Kpn*I/*Xho*I restriction sites.

The following primers were used:

ATMcKpn1F-5'-GGTGGTACCATGGGAGAATATGGAAATCTGGTG3'
ATMcXho1R-5'CTCCTCGAGTCAAGCTTCAAAGGATTGTCATGGTC-3'

The recombinant SFB-ATM kinase domain (SFB-ATM_K) was pulled down using streptavidin beads from pcDNA-SFB-ATM_K-transfected HEK293 cells and eluted in kinase buffer (20 mM HEPES, 10 mM MgCl₂, 1 mM DTT and 20 ng BSA) supplemented with 2 mg/ml biotin. Streptavidin pull-down using pcDNA-SFB-transfected cell lysate was taken as control. The kinase assay was performed as follows: 20 µl of SFB-ATM_K, 300 ng of DNMT2 and 1 µl of γ^{32} P-ATP were taken to give a 30 µl reaction mixture, which was incubated for 30 min at 30°C. Substrate blank (-DNMT2) and kinase blank (-ATM_K) were taken as control. The reaction mix was resolved on SDS-PAGE, the gel was stained in Coomassie blue stain, vacuum-dried, exposed overnight and scanned in a phosphorimager (Fuji Film FLA-9000).

Mass spectrometry analysis

DNMT2 was phosphorylated by SFB-ATM kinase in an *in vitro* kinase assay as mentioned above. For MS/MS analysis, the kinase assay was performed with 10 mM ATP instead of γ^{32} P-ATP. The reaction was resolved on 10% SDS-PAGE followed by Coomassie blue staining. The DNMT2 protein band was excised and sent for MS/MS analysis of phospho-DNMT2 at Taplin Mass Spectrometry Facility at Harvard Medical School, U.S.A. The phosphorylation score was calculated as an 'A' score [30].

Source of antibodies used

Antibodies against DNMT2 (sc-365001, sc-20702) were purchased from Santa Cruz. Antibodies against phosphoserine (05-1000) were purchased from Millipore. Anti-G3BP (ab56574) was purchased from Abcam. Alexa Fluor 488 (A11078) and Alexa Fluor 568 (A11061) antibodies were purchased from Invitrogen.

Results

DNMT2 re-localizes to SGs in response to multiple cellular stresses including HIV-1 infection

Previous work from our laboratory had shown DNMT2 to be a component of SGs [11]. DNMT2 not only re-localized to cytoplasmic SG in response to oxidative and endoplasmic reticulum (ER) stress, but it was also found to be interacting and co-localizing with established SG markers like G3BP and TTP [1,11]. This re-localization is not just restricted to oxidative and ER stress, as we find re-localization of DNMT2 to the cytoplasmic SGs even under other stress conditions including low pH and osmotic shock (Supplementary Figure S1).

In the previous study, we had noted that several genes involved in host defence against viral infection were misregulated upon DNMT2 overexpression [11]. Since infection by a pathogen also causes stress to the cell, we sought to investigate whether infection of a cell by a virus could also cause DNMT2 re-localization. CEMx174

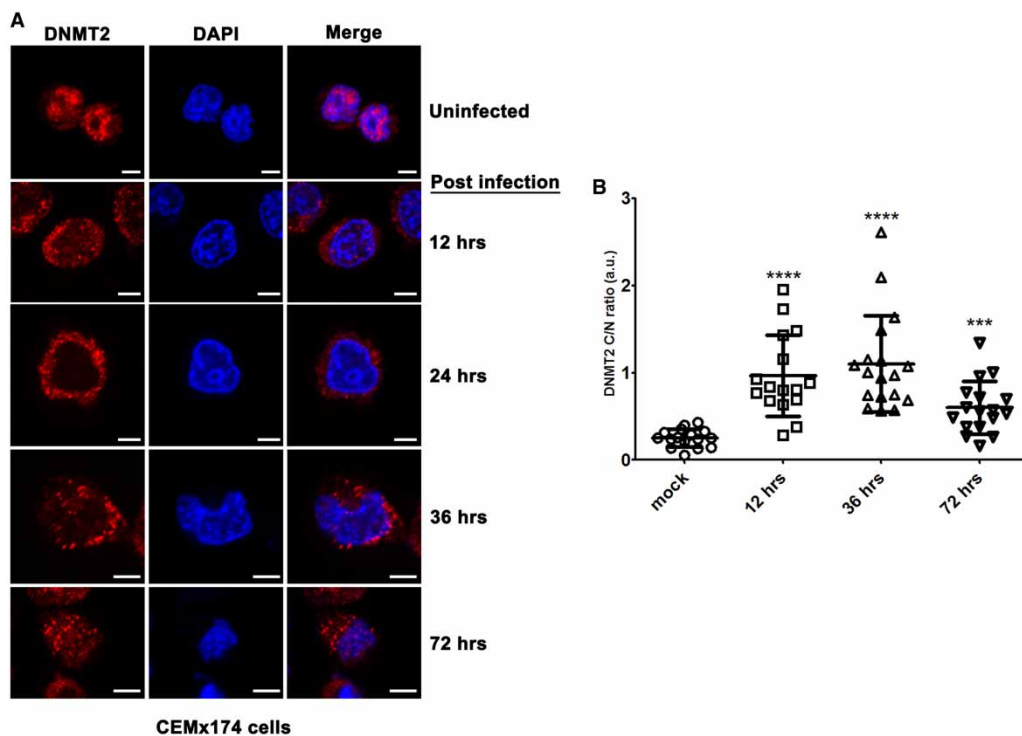


Figure 1. Re-localization of DNMT2 in response to HIV-1 infection.

(A) Localization of endogenous DNMT2 was examined by immunostaining in uninfected and at various time points post HIV-1 infection. Note the dynamic change in localization of endogenous DNMT2 during HIV-1 infection. Nucleus was counterstained with DAPI. Scale bar — 5 μ M. (B) Cytoplasm/nuclear (C/N) ratio for the DNMT2 signal in mock-infected and HIV-1-infected CEMx174 cells. The intensity of nuclear and cytoplasmic immunofluorescence was calculated using Image J ($n = 16$). Error bars represent the standard deviation (SD). * indicates significant difference Student's *t*-test, *** $P < 0.001$, **** $P < 0.0001$. a.u., arbitrary units.

cells were infected with HIV-1 and the localization of the endogenous DNMT2 was observed at different time intervals by immunofluorescence, 12–72 h post-infection (see Materials and Methods). We observed dynamic re-localization of the DNMT2 protein from the nucleus to the cytoplasmic SGs. DNMT2 was found to be predominantly nuclear in uninfected cells (Figure 1A, topmost panel). By 12 h, DNMT2 was found to be present both in the cytoplasm and the nucleus (Figure 1A, second panel from top). Twenty-four hours after infection, DNMT2 was completely re-localized to the cytoplasmic SGs. The predominant cytoplasmic localization persisted till 36 h post-infection and by 72 h, DNMT2 was found both in the cytoplasm and the nucleus (Figure 1A). The quantitation of the DNMT2 signal in uninfected and HIV-1-infected CEMx174 cells also confirmed significant localization of DNMT2 in the cytoplasm after HIV-1 infections (Figure 1B). As a control, to confirm that the DNMT2 re-localization was correlated with HIV-1 infection, the cells were incubated with heat-killed HIV viral particles. No re-localization of DNMT2 was observed in these cells infected with heat-killed HIV viral particles (Supplementary Figure S2). The re-localization of DNMT2 upon HIV-1 infection was also true in another cell line, SupT1 (Supplementary Figure S3). To confirm that the DNMT2 cytoplasmic foci were indeed SGs, the HIV-1-infected cells were also immunostained for G3BP, a known SG marker [1]. As can be seen in Supplementary Figure S3, upon HIV-1 infection, DNMT2 does co-localize with G3BP foci in the cytoplasm. Thus, the DNMT2 protein responds to multiple cellular stresses including HIV-1 infection and gets localized to the SGs.

Re-localization of DNMT2 is dependent on its phosphorylation by ATM kinase

DNMT2 does not have any canonical nuclear export signal. As many nuclear proteins that are involved in RNA processing show phosphorylation-/dephosphorylation-dependent cytoplasmic re-localization, we

decided to examine whether DNMT2 localization was also dependent on phosphorylation [31]. DNMT2 was immunoprecipitated from untreated or sodium arsenite (oxidative stress)-treated HEK293 cells followed by western blotting and probed with phosphoserine antibodies. Indeed, the immunoprecipitated DNMT2 was found to be phosphorylated at serine residue(s) in response to oxidative stress (Figure 2A). Bioinformatic investigation, using web-based search engine (PhosphoMotif Finder) that can predict probable kinases involved in phosphorylation at specific sites, indicated the ATM kinase to be the probable kinase for

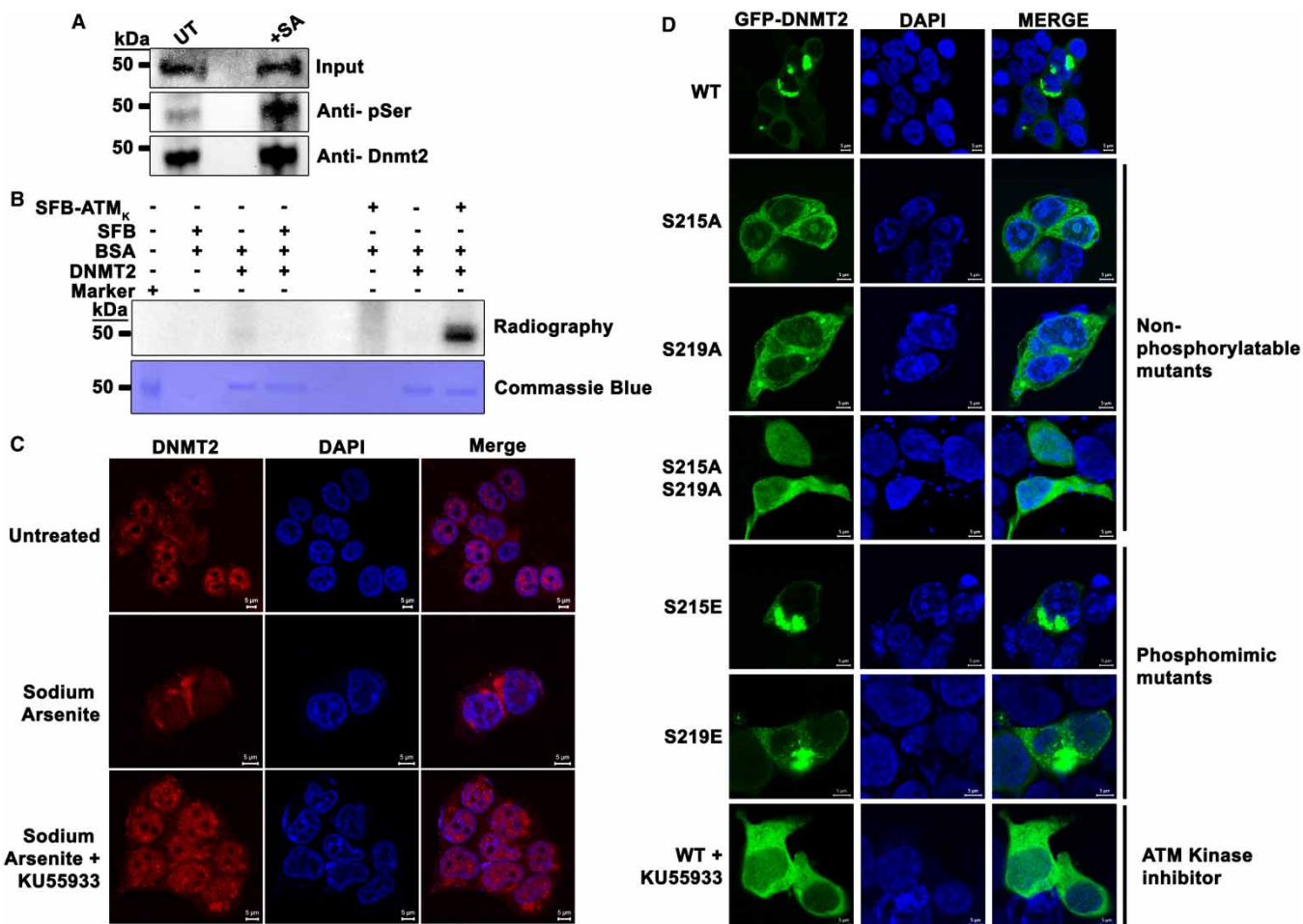


Figure 2. Re-localization of DNMT2 to stress granules is dependent on its phosphorylation by ATM kinase.

(A) DNMT2 gets phosphorylated at serine residues in response to oxidative stress. DNMT2 immunoprecipitated from control and sodium arsenite-treated cells using DNMT2 antibody was probed for serine phosphorylation with phosphoserine antibody (anti-pSer). UT, untreated cells; +, SA; -, sodium arsenite-treated cells. The blot was also probed with DNMT2 antibody as a control. (B) *In vitro* kinase assay showing ATM kinase-mediated phosphorylation of DNMT2. SFB-tagged ATM kinase domain (SFB-ATM_K) was pulled down from SFB-ATM_K-transfected cells and incubated with purified recombinant 6×His-DNMT2 (DNMT2) protein in the presence of γ^{32} P-ATP. As a control, protein(s) pulled down from pcDNA-SFB-transfected cells were also incubated with 6×His-DNMT2. Incubation of SFB-ATM_K pull-down fraction with BSA alone was also used as control. Note that the transfer of γ^{32} P to DNMT2 occurs only in the presence of SFB-ATM kinase. Upper panel, autoradiograph showing the phosphorylation of DNMT2 by the ATM kinase domain. Coomassie blue staining in the lower panel shows the total amount of 6×His-DNMT2 in various reactions. (C) ATM kinase inhibitor prevents re-localization of DNMT2 in response to stress. HEK293 cells were treated with sodium arsenite in the absence (middle panel) or presence of ATM kinase inhibitor KU55933 (lower panel) and immunostained for endogenous DNMT2. Nuclei were counterstained with DAPI. Scale bar – 5 μ M. (D) Serine residues at S215 and S219 are involved in the re-localization of DNMT2. HEK293 cells were transfected with either the WT, non-phosphorylatable (S215A, S219A or S215A/S219A) or phosphomimetic (S215E or S219E) mutants of GFP-DNMT2. GFP-DNMT2-transfected HEK293 cells were also treated with ATM kinase inhibitor KU55933 (lowermost panel). Nuclei were counterstained with DAPI. Scale bar – 5 μ M.

DNMT2 phosphorylation [32]. To examine if indeed ATM kinase was involved in DNMT2 phosphorylation, recombinant SFB-tagged ATM kinase domain (SFB-ATM_K) was purified from HEK293 cells and incubated with *Escherichia coli* purified recombinant 6×His-DNMT2 in an *in vitro* kinase assay using $\gamma^{32}\text{P}$ -ATP as a phosphate donor (see Materials and Methods). As a control, 6×His-DNMT2 was also incubated with the SFB tag alone (purified from HEK293 cells). As a negative control, SFB-ATM_K was also incubated with BSA. While SFB-ATM_K transferred a phosphate group to DNMT2, DNMT2 was not phosphorylated by the SFB tag alone (Figure 2B). Moreover, SFB-ATM_K did not phosphorylate BSA. MS/MS mass spectrometry analysis on recombinant 6×His-DNMT2 incubated with ATM kinase in an *in vitro* kinase assay showed serine at position 215 and 219 to be phosphorylated (Supplementary Figure S4). Furthermore, in an *in vitro* kinase assay, DNMT2 phosphorylation by SFB-ATM_K was found to be impaired in the presence of the ATM kinase inhibitor KU55933 (Supplementary Figure S5). This suggested that DNMT2 was being phosphorylated by ATM kinase.

To test the possibility that cytoplasmic re-localization of DNMT2 upon stress was dependent on phosphorylation by ATM kinase, HEK293 cells were treated with ATM kinase inhibitor KU55933 followed by incubation with sodium arsenite (oxidative stress). Treated or untreated cells were immunostained for DNMT2. Endogenous DNMT2, which re-localizes to cytoplasmic SGs in response to oxidative stress, was found to be restricted to the nucleus even after sodium arsenite treatment in the presence of KU55933 (Figure 2C and Supplementary Figure S6). These observations indicated that re-localization of endogenous DNMT2 from the nucleus to the cytoplasm upon stress was dependent on its phosphorylation by ATM kinase.

We had previously shown that when GFP-DNMT2 is overexpressed in mammalian cells, it localizes to cytoplasmic SGs and mimics the localization of endogenous DNMT2 during stress [11]. To examine whether this transfected DNMT2 protein was phosphorylated, the SFB-DNMT2 fusion protein construct was transfected into HEK293 cells. The SFB-DNMT2 fusion protein, pulled down using biotin and probed with phosphoserine antibody, was found to be phosphorylated (Supplementary Figure S7). To examine the role of the two serine residues S215 and S219 found to be phosphorylated in DNMT2 during stress, these serine residues were mutated to alanine independently as well as together (GFP-DNMT2^{S215A}, GFP-DNMT2^{S219A} and GFP-DNMT2^{S215A+S219A}) in the GFP-DNMT2 construct by site-directed mutagenesis, to create non-phosphorylatable mutants. Upon transfection of these constructs into HEK293 cells, the cytoplasmic localization of overexpressed mutant GFP-DNMT2 was affected to varied extents in the mutants. GFP-DNMT2^{S215A} and GFP-DNMT2^{S219A} showed localization in the nucleoli in addition to the cytoplasm. On the other hand, the GFP-DNMT2^{S215A+S219A} double mutant, in contrast with the GFP-DNMT2 (WT, wild type), was localized to the nucleus in addition to the cytoplasm (Figure 2D) as is the case with endogenous DNMT2 (Figure 2C, upper panel). The localization of GFP-DNMT2^{S215A+S219A} double mutant was also similar to that of WT GFP-DNMT2 in HEK293 cells that were treated with the ATM kinase inhibitor KU55933 (Figure 2D, lowest panel). As a control, GFP-DNMT2^{S215E} and GFP-DNMT2^{S219E} phosphomimetic mutants of GFP-DNMT2 were also tested for their localization. Both these phosphomimetic mutants of GFP-DNMT2 were found to be localized predominantly in the cytoplasm as was observed for GFP-DNMT2 (Figure 2D). This would indicate that phosphorylation of serine residues at the 215 and 219 positions in DNMT2 have an important role to play in its re-localization to the cytoplasm.

DNMT2 binds to mRNA

In our previous study, we had observed co-localization of DNMT2 with mRNA in the SGs using cDNA, corresponding to the whole-cell mRNA, as a probe [11]. This would suggest that DNMT2 could also be interacting with different mRNA species present in the SGs. Therefore, we decided to characterize the RNA-binding potential of DNMT2 by the RNA pull-down assay. DNMT2-bound RNA was enriched from total RNA isolated from HEK293 cells treated with sodium arsenite (oxidative stress) by incubating with recombinant 6×His-DNMT2 protein bound to Ni-NTA agarose beads. A few RNA species that were present in the bound fraction of the sodium arsenite-treated samples were identified to be regions within the BRWD1 (Bromodomain and WD repeat domain containing 1, transcript variant 2), RPL27A (ribosomal protein L27A), CNNM3 (cyclin M3) and the non-coding (4(A+3)1) mRNAs (see Supplementary Information for experimental details and Supplementary Figure S8). To confirm the interaction of DNMT2 with these mRNA species, RNA-EMSA (electrophoretic mobility shift assay) was performed with recombinant DNMT2 and $\alpha^{32}\text{P}$ -CTP-labelled *in vitro* RNA probes for 4(A+3)1 and BRWD1, RPL27A. Since tRNA^{Val} is a known substrate for DNMT2 [16], binding with tRNA^{Val} was taken as a positive control. DNMT2 showed efficient binding with all the mRNA probes (Figure 3A).

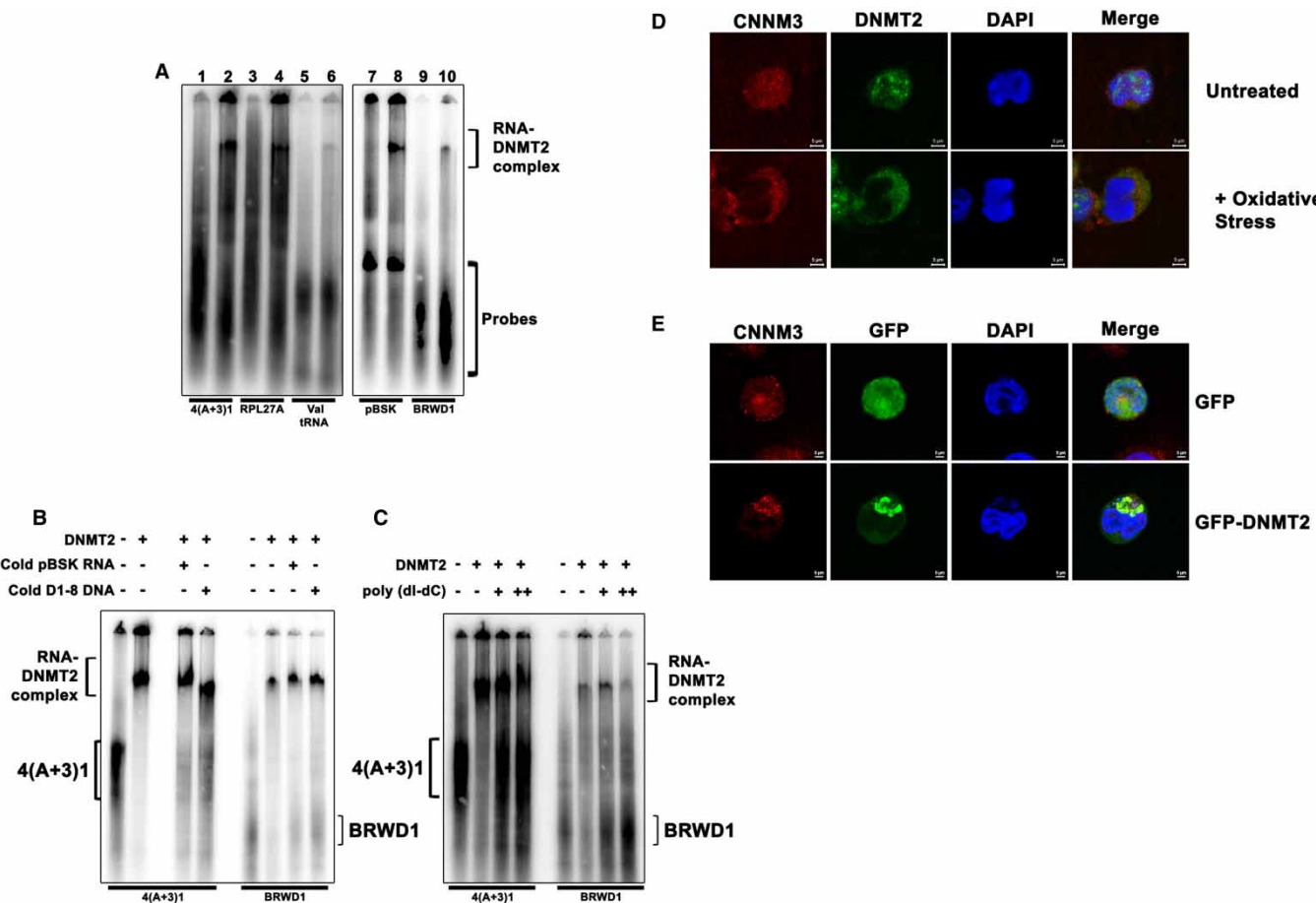


Figure 3. DNMT2 binds to and co-localizes with mRNA in stress granules.

(A) DNMT2 binds to mRNA *in vitro*. RNA-EMSA showing binding of DNMT2 with different *in vitro*-transcribed mRNA species (indicated below the image). Lanes 1, 3, 5, 7 and 9 — radiolabelled probes corresponding to the indicated *in vitro*-transcribed mRNA species. Lanes 2, 4, 6, 8 and 10 — radiolabelled probes + DNMT2 protein. Note that DNMT2 also binds to *in vitro* RNA transcribed from pBSK cloning vector. (B and C) DNMT2 binds more strongly to mRNA. RNA-EMSA with recombinant 6xHis-DNMT2 protein and radiolabelled *in vitro*-transcribed RNA, corresponding to regions within 4(A+3)1 and BRWD1 mRNA, as probes. Unlabelled *in vitro*-synthesized pBSK RNA, DNA-specific to the D1-8 DNA fragment (see Supplementary Information) (B) and poly (dI-dC) (C) were used as cold competitor. + indicates the presence and – indicates the absence of the indicated component in the RNA-protein-binding reaction. + is 10 \times and ++ is 100 \times for poly (dI-dC) in (C). (D and E) DNMT2 and mRNA species co-localize in stress granules during oxidative stress. RNA-FISH was performed using Alexa Fluor 546-labelled CNNM3 mRNA probe on: HEK293 cells untreated (upper panel) or treated (lower panel) with sodium arsenite (oxidative stress) and immunostained for endogenous DNMT2 (D); and HEK293 cells transfected with either GFP (upper panel) or GFP-DNMT2 (lower panel) (E). Nuclei were counterstained with DAPI. Scale bar — 5 μ M.

We next sought to investigate whether DNMT2 had substrate specificity for a specific mRNA species. Furthermore, as DNMT2 also has binding affinity for DNA (Supplementary Figure S9), we were also interested in examining the mRNA-binding specificity of DNMT2 when compared with DNA [33]. Therefore, RNA-EMSA was performed with *in vitro*-transcribed mRNA corresponding to regions within the 4 (A+3)1 and BRWD1 genes (see above) in the presence or absence of non-specific and non-radioactive mRNA (pBSK; cold competitor) and DNA fragment D1-8 (see Supplementary Information) or poly (dI-dC). Unlabelled mRNA and DNA competitor were used at concentrations of 25 \times and 10 \times respectively, whereas poly (dI-dC) was used at 10 \times and 100 \times . In the presence of DNA or poly (dI-dC) as cold competitor, the intensity of the RNA-DNMT2 complex was reduced but not abolished (Figure 3B,C). This indicated that DNMT2 has a preference for RNA over DNA as a substrate.

10× pBSK mRNA was also not able to compete out binding with 4 (A+3)1 and BRWD1 mRNA (Figure 3B). This could indicate the specificity of DNMT2 for specific mRNA species. However, when RNA-EMSA was performed using an $\alpha^{32}\text{P}$ -labelled non-specific RNA (pBSK MCS transcribed from T7 promoter), DNMT2 showed binding to pBSK RNA. This could suggest that the DNMT2 could bind to any RNA species but had stronger affinity to specific mRNA species.

DNMT2 co-localizes with mRNA species during stress

DNMT2 is a component of the SGs during stress [11]. To examine whether any of the above-mentioned mRNA species also co-localize with DNMT2 during stress, fluorescence RNA *in situ* hybridization using fluorescent probe against CNNM3 and RPL27A mRNA followed by immunostaining for endogenous DNMT2 was performed on HEK293 cells untreated or treated with sodium arsenite. CNNM3 and RPL27A mRNAs are normally localized both in the nucleus and the cytoplasm, but during stress conditions both these mRNA species were present along with endogenous DNMT2 predominantly in the cytoplasm (Figure 3D and Supplementary Figure S10).

We had previously shown that upon overexpression, GFP-DNMT2 localizes to the SGs ([11] and Figure 2D). Fluorescence RNA *in situ* hybridization for CNNM3 mRNA in GFP-DNMT2-expressing HEK293 cells showed co-localization of GFP-DNMT2 with CNNM3 in the cytoplasm (Figure 3E). This was also true for RPL27A (Supplementary Figure S10). This indicated that DNMT2 co-localizes with mRNA species in the SGs during stress.

DNMT2 interacts with HIV-1 RNA during infection

As observed for other environmental stress conditions, DNMT2 also re-localizes to SGs during HIV-1 infection (Figure 1A and Supplementary Figure S3). Since HIV uses the host machinery to transcribe its own transcripts and because the HIV RNA goes through the same RNA-processing machinery as host mRNA, the HIV RNA transcribed inside the host cell has all the hallmarks of host mRNA [34]. Moreover, it is known that HIV infection induces SG formation with HIV-2 RNA being found localized to SGs during infection [35]. In light of our finding that DNMT2 could bind mRNA species during stress, we examined the possibility that DNMT2 could also interact with HIV-1 RNA during infection. To achieve this, affinity RNA pull-down was performed, using recombinant 6×His-DNMT2, on total RNA isolated from HIV-1-infected SupT1 cells followed by semi-quantitative RT-PCR for a region within the *nef* gene of HIV-1 RNA. As can be seen from Figure 4A, 6×His-DNMT2 binds HIV-1 RNA. The binding of HIV-1 RNA to DNMT2 was further confirmed by performing RNA-EMSA using 6×His-DNMT2, $\alpha^{32}\text{P}$ -CTP-labelled and *in vitro*-transcribed probes from H18 (corresponding to *nef* gene, Figure 4B), H9 (present within the *integrase* gene, Supplementary Figure S11) and H13 (present within a region that is part of the *vpu*, *rev*, *env* and *tat* genes, Supplementary Figure S11) regions of the HIV-1 RNA. To examine whether HIV-1 RNA and DNMT2 co-localize during infection, RNA fluorescence *in situ* hybridization (for the H18 region) followed by immunostaining for DNMT2 was performed on SupT1 cells, 24–72 h after infection. As can be seen in Figure 4C, HIV-1 RNA and DNMT2 indeed co-localize. To confirm that the localization of HIV-1-RNA and DNMT2 was within the cytoplasmic SGs, RNA-FISH and immunostaining were also performed for HIV-1 and DNMT2, respectively, along with immunostaining for the well-established SG marker, G3BP, in SupT1 cells. HIV-1 RNA was found to co-localize with DNMT2 and G3BP (Supplementary Figure S12), indicating that HIV-1 RNA indeed localizes to SGs along with DNMT2 and G3BP.

DNMT2 mediates mRNA cytosine methylation in response to stress and HIV-1 RNA during infection

DNMT2 has been shown to methylate tRNA. To test the possibility that the DNMT2 was methylating mRNA in response to stress, we sought to examine the methylation status of RPL27A, CNNM3 and BRWD1 mRNA. Similarly, to investigate whether DNMT2 could methylate HIV-1 RNA during infection, the methylation status of the H18 region within the *nef* gene of HIV-1 RNA was tested by *in vitro* and *in vivo* methylation assays.

In the *in vitro* RNA methylation assay (filter binding), *in vitro*-transcribed RPL27A, CNNM3, BRWD1 mRNA and H18 region of HIV-1 RNA were used as substrates with tritiated SAM as a methyl donor. As a positive control, *in vitro*-transcribed tRNA^{Val} was also used as a substrate. As can be seen in Figure 5A, all mRNAs and HIV-1 RNA substrates showed significant gain of tritiated methyl groups in the presence of

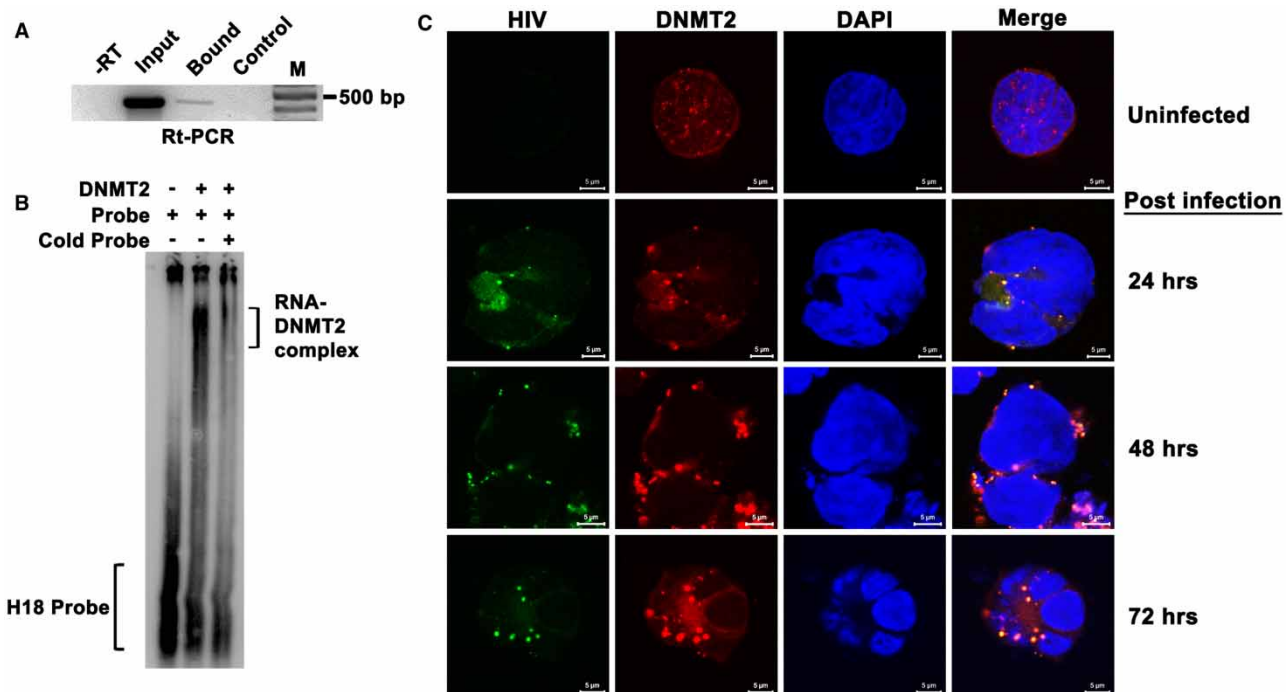


Figure 4. DNMT2 binds to and co-localizes with HIV-1 RNA during infection.

(A) Representative RT-PCR showing DNMT2 binding to HIV-1 RNA *in vivo*. RNA pull-down assay performed on total cell RNA from HIV-1-infected SupT1 with recombinant 6xHis-DNMT2 followed by semi-quantitative RT-PCR for the H18 region within the *nef* gene. -RT denotes RT-PCR without the addition of template; Bound – RT-PCR on SFB-DNMT2-bound RNA fraction; Control – RT-PCR on SFB-bound RNA; M – 100 bp DNA marker. (B) RNA-EMSA showing DNMT2 binding with *in vitro*-transcribed HIV-1 RNA. Radiolabelled and *in vitro*-transcribed RNA for the H18 region (from within the *nef* gene of HIV RNA) was incubated with DNMT2 in the presence or absence of unlabelled *in vitro*-synthesized H18 RNA (100 \times). + indicates the presence and – indicates the absence of the indicated component in the RNA–protein-binding reaction. (C) DNMT2 co-localizes with HIV-1 RNA during infection. RNA-FISH was performed on uninfected and HIV-1-infected (at the indicated times post-infection) SupT1 cells with the Cy3-labelled H18 region RNA probe (corresponding to the *nef* gene in the HIV-1 RNA; see Materials and Methods) and immunostained for endogenous DNMT2. HIV-1 RNA (green) co-localizes with DNMT2 (red) in the SGs. Nuclei were counterstained with DAPI. Scale bar – 5 μ m.

recombinant DNMT2, which was comparable to that observed for tRNA^{Val}, which is a known substrate of DNMT2.

To examine the nature of this methylation, the DNMT2-mediated methyltransferase assay was performed on *in vitro*-transcribed RPL27A mRNA and the H18 region of HIV RNA followed by RNA-specific bisulphite sequencing. When compared with the RNA substrates incubated with BSA, significant higher numbers of cytosines both at CpG and non-CpG dinucleotides were found to be methylated in the presence of DNMT2 for both RPL27A (Figure 5B,D) and the H18 region of HIV-1 (Figure 5C,E).

To test whether DNMT2 methylates RPL27A, CNNM3 and BRWD1 mRNA *in vivo*, we performed MeRIP-RT-PCR (methylated RNA immunoprecipitation RT-PCR) using the 5-methyl cytosine (5mC) antibody [36]. RNA bound to DNMT2, isolated from sodium arsenite-treated HEK293 cells that were transiently transfected with SFB-DNMT2, was pulled down using 5mC antibody followed by RT-PCR for RPL27A, BRWD1 and CNNM3. All these mRNAs were enriched in the methylated bound fraction of SFB-DNMT2-transfected HEK293 cells but not in the control bound fraction from SFB-transfected HEK293 cells (Figure 5F).

The status of HIV RNA methylation *in vivo* upon HIV-1 infection was also examined by MeRIP-RT-PCR for HIV-1 RNA. DNMT2-associated RNA was pulled down from HEK293T cells, co-transfected with SFB-DNMT2 and pNL4.3, followed by MeRIP and semi-quantitative RT-PCR. HIV-1 RNA was enriched in the bound fraction of SFB-DNMT2/pNL4.3-transfected HEK293T cells (Figure 5G), indicating DNMT2-mediated HIV-1 RNA methylation during infection.

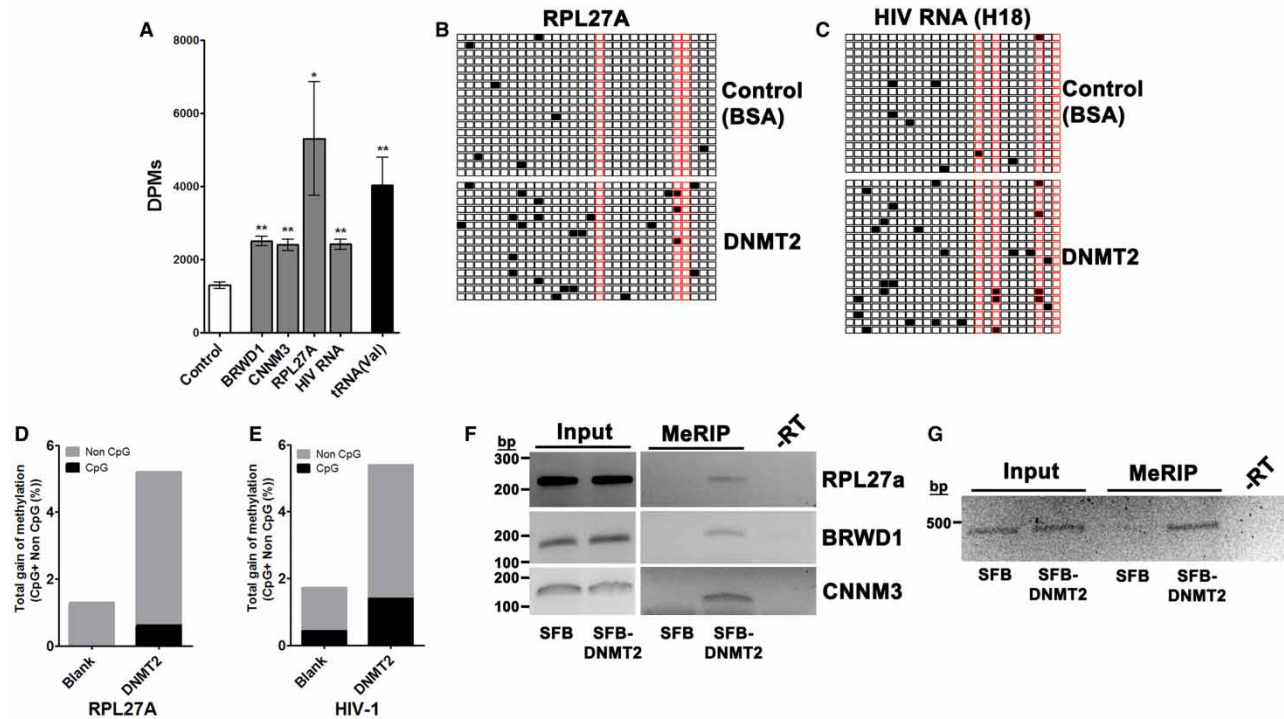
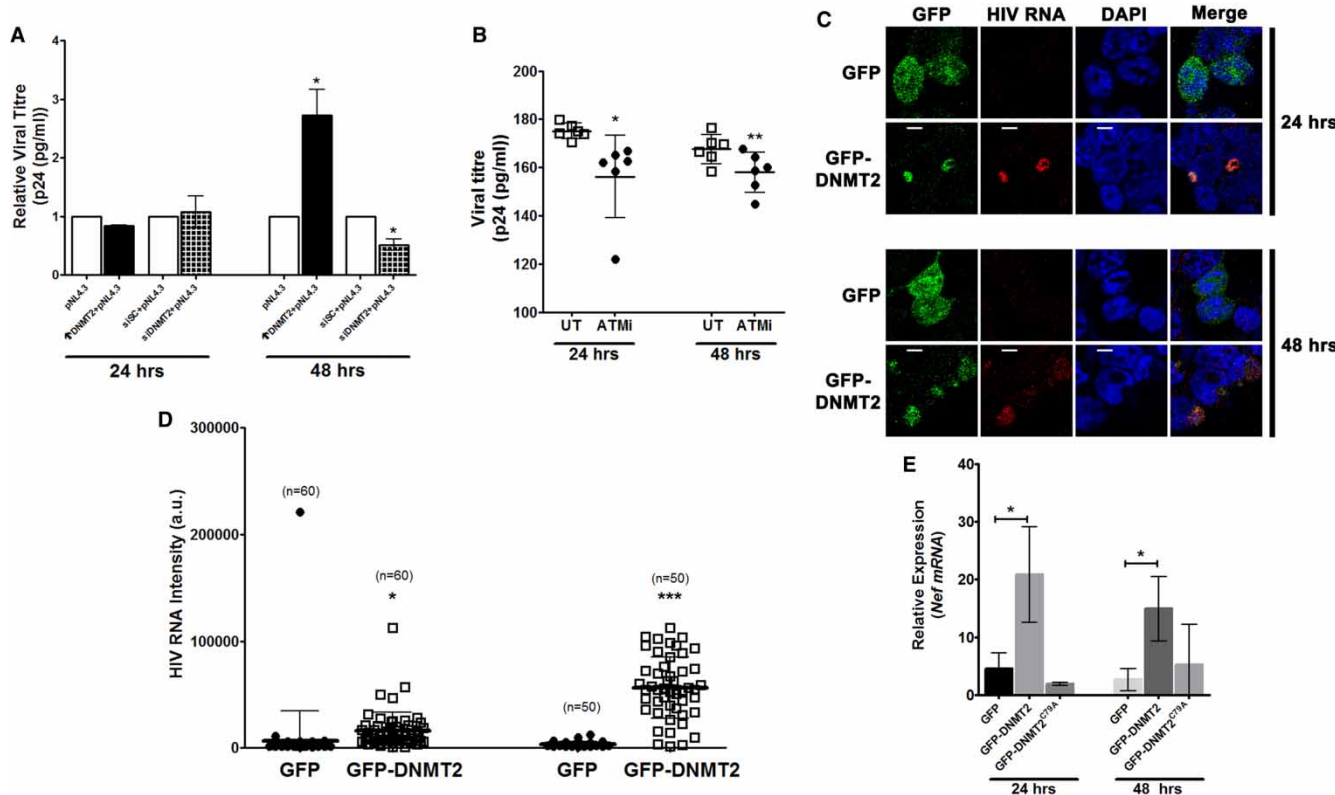


Figure 5. DNMT2 can methylate mRNA and HIV RNA.

(A) *in vitro* methylation assay. Filter binding assay was performed on indicated *in vitro*-transcribed mRNA, HIV-1 RNA and Valine tRNA species with DNMT2 in the presence of tritiated SAM. Control – BSA. Error bars represent the standard deviation (SD). * indicates significant difference Student's *t*-test, ***P* < 0.005; **P* < 0.01. (B and C) Bisulphite sequencing analysis on *in vitro*-transcribed and methylated RPL27A RNA (B) and H18 region of HIV-1 RNA (C). The position of each cytosine as it appears in the sequence is represented as a rectangle. Red rectangles indicate cytosine in CpG and black rectangles indicate cytosine in a non-CpG dinucleotide context. Filled symbols indicate methylated cytosine. (D and E) Quantification of percentage gain of methylated cytosines [CpG + non-CpG (%)] in RPL27A (D) and HIV-1 RNA (E) after bisulphite sequencing. (F) Representative MeRIP-RT-PCR (semi-quantitative) for RPL27A, BRWD1, CNNM3 mRNA. DNMT2-bound RNA was enriched from SFB-DNMT2-transfected HEK293 cells followed by MeRIP. MeRIP on HEK293 cells transfected with pcDNA-SFB followed by sodium arsenite treatment was taken as a negative control. -RT denotes RT-PCR without the addition of template. (G) Representative MeRIP-RT-PCR (semi-quantitative) for the H18 region of HIV-1 RNA. DNMT2-bound RNA was enriched from pNL4.3 and SFB-DNMT2-co-transfected HEK293 cells followed by MeRIP. MeRIP on uninfected HEK293 cells transfected with pcDNA-SFB alone was taken as a negative control. -RT denotes RT-PCR without the addition of template RNA.

DNMT2 facilitates HIV-1 infection

To test whether the DNMT2-mediated methylation of HIV-1 RNA during infection was indicative of a role for DNMT2 in host cellular response to HIV-1 infection, we examined the efficacy of HIV-1 infection in the presence of higher (overexpression) or lower (knockdown, Supplementary Figure S13) levels of DNMT2. HEK293T cells were transiently co-transfected with (i) pNL4.3/SFB-DNMT2 (overexpression); (ii) pNL4.3/pcDNA-SFB (overexpression control); (iii) pNL4.3/siRNA-DNMT2 (down-regulation, Supplementary Figure S10); and (iii) pNL4.3/scrambled siRNA (siRNA control, Supplementary Figure S13). p24 ELISA that detects p24 HIV capsid protein (p24 is an HIV capsid protein that is widely used as the marker for HIV infections) was performed on cell supernatant, 24 and 48 h after infection. Twenty-four hours post-infection, the p24 levels were similar for all the transfected cells. However, a significant difference in the viral titre was observed in SFB-DNMT2-overexpressing and DNMT2-knockdown cells when compared with the control, 48 h post-infection (Figure 6A). HEK293T cells overexpressing SFB-DNMT2 showed a two-fold increase in viral titre, whereas HEK293T cells with DNMT2 down-regulation showed a significant decrease in the viral titre (p24 level). This was quite surprising as this indicated that DNMT2 was facilitating HIV particle production.

**Figure 6. DNMT2 promotes HIV infection.**

(**A**) DNMT2 expression level affects the HIV-1 viral titre. HIV-1 packaging plasmid pNL4.3 was co-transfected into HEK293T cells with either pcDNA-GFP-DNMT2 (black bars) or siRNA against DNMT2 (bars with square pattern, see Materials and Methods). The level of the viral p24 protein was measured at indicated time points in the cell supernatant. The level of the viral p24 protein in HEK293 cells co-transfected with pNL4.3 & pcDNA-GFP and pNL4.3 & scrambled siRNA was used as a control for the analysis. (**B**) ATM kinase inhibitor affects the HIV-1 p24 levels. SupT1 cells were treated with ATM kinase inhibitor (filled circles), KU55933, following which they were infected with HIV-1. The level of the viral p24 protein was measured at indicated time points in the cell supernatant. Open squares, SupT1 cells not incubated with KU55933. (**C** and **D**) DNMT2 stabilizes HIV-1 RNA during infection. mRNA transcription was blocked in pNL4.3/GFP-DNMT2 or pNL4.3/GFP-transfected HEK293T cells with Actinomycin D. (**C**) Representative FISH images showing the intensity of HIV-1 RNA in Actinomycin D-treated and untreated transfected cells at 24 h (upper panel) and 48 h (lower panel). Nuclei were counterstained with DAPI. Scale bar — 5 μ M. (**D**) Quantification of the HIV-1 RNA-FISH signal for the indicated number of untreated and Actinomycin D-treated cells by scatter plot analysis. Signal intensity was calculated for the indicated number of cells ($n > 50$ across more than eight randomly chosen fields for each time point), 24 and 48 h post-transfection. (**E**) Quantitative real-time RT-PCR to determine the HIV-1 RNA load. HEK293T cells transfected with pNL4.3/GFP, pNL4.3/GFP-DNMT2 or pNL4.3/GFP-DNMT2^{C79A} (catalytically inactive mutant of GFP-DNMT2) were treated with Actinomycin D. Quantitative RT-PCR was performed on total RNA isolated from these cells 24 and 48 h after transfection. Error bars represent the standard deviation (SD). * indicates significant difference Student's *t*-test, **P* < 0.05; ***P* < 0.005; ****P* < 0.001.

DNMT2 co-localizes with HIV-1 RNA in SGs during infection (Figure 4 and Supplementary Figure S12) and, as shown in Figure 2C, re-localization of DNMT2 from the nucleus to the SGs was blocked when its phosphorylation was inhibited by the ATM kinase inhibitor KU55933. Therefore, to confirm the role of DNMT2 in HIV-1 particle production, we examined the HIV-1 viral titre (p24 capsid protein levels) in the presence of KU55933. SupT1 cells were treated with KU55933 following which they were infected with HIV-1 (see Materials and Methods). P24 ELISA was performed on cell supernatant, 24 and 48 h after infection. A significant decrease in the viral titre was observed in KU55933-treated cells when compared with the control untreated cells, at both 24 and 48 h time points post-infection (Figure 6B). ATM kinase is expected to affect the activity of several downstream proteins, which in turn could lead to a reduction in the viral titre. To examine whether the effect of ATM kinase on HIV titre was through DNMT2 phosphorylation, we performed p24 ELISA on HEK293T cells, transfected with either pNL4.3 and DNMT2 siRNA or pNL4.3 and scrambled

siRNA, and treated with KU55933 (see Materials and Methods). Untreated transfected cells were taken as control. As can be seen in Supplementary Figure S14, no further reduction in viral titre was observed even after the addition of KU55933 in DNMT2-knockdown cells. This confirmed our finding that DNMT2 was facilitating HIV particle production.

DNMT2 provides post-transcriptional stability to HIV RNA

An increased level of HIV-1 viral titre in the presence of DNMT2 indicated that the virus was utilizing the host-encoded DNMT2 for promoting its own survival and growth. Could the methylation of HIV-1 RNA by DNMT2 be improving its survivability in the cell? To examine the possibility that the increased viral titre was because of increased stability of HIV-1 RNA in the presence of DNMT2, RNA-FISH for HIV-1 RNA was performed on GFP/pNL4.3 and GFP- DNMT2/pNL4.3-co-transfected HEK293T cells. Actinomycin D (5 µg/ml) was added to the culture medium 12 h after transfection and the cells were visualized 24 and 48 h after transfection by confocal microscopy, and the intensity of the HIV-1 RNA signal for multiple cells in randomly selected fields was quantified. As can be seen in Figure 6C,D, the intensity of HIV-1 RNA staining was higher in a significantly higher number of GFP-DNMT2/pNL4.3-transfected HEK293T cells when compared with control GFP/pNL4.3-transfected cells. To further confirm the effect of DNMT2 on HIV-1 RNA stability, HEK293T cells, co-transfected either with pNL4.3 and GFP, pNL4.3 and GFP-DNMT2 or pNL4.3 and a catalytically inactive mutant of DNMT2, GFP-DNMT2^{C79A} were treated with Actinomycin D. Quantitative RT-PCR performed for HIV-1 RNA on these cells showed that the level of HIV-1 RNA (*nef* mRNA) was significantly higher in the presence of GFP-DNMT2. The catalytically inactive GFP-DNMT2^{C79A} had no effect on the stability of HIV-1 RNA (Figure 6E).

To investigate the possibility that DNMT2 also provides post-transcriptional stability to mRNA molecules, RNA-FISH was performed for RPL27A on sodium arsenite-treated GFP and GFP-DNMT2-transfected HEK293 cells that were subsequently grown in the presence of Actinomycin D. Quantification of the intensity of the RPL27A mRNA signal (for multiple cells in randomly selected eight fields) at 0, 2 and 4 h post-Actinomycin D addition showed higher intensity in a significantly higher number of GFP-DNMT2-transfected cells (Supplementary Figure S15).

Discussion

With different functions being ascribed in different species, the evolutionarily conserved DNMT2 has remained an enigmatic methyltransferase in terms of its function [15,37].

Though previous studies have shown tRNA methylation capability of DNMT2 in several species, DNMT2 has also been shown to have residual DNA methylation activity [14–16]. In this study, we add mRNA to the list of DNMT2 substrates and show that DNMT2 methylates mRNA. Importantly, we show that HIV uses the RNA methylation property of DNMT2 to stabilize its RNA genome during viral production, which in turn may facilitate it to proliferate and survive in the host cell.

DNMT2 binds and methylates mRNA

Epigenetic modification of RNA is being recognized as an important event during RNA metabolism [38–40]. As SGs are cytoplasmic loci where several untranslated RNA species are brought in and sorted either for decay or storage during environmental stress, it is possible that RNA epigenetic modifications play a role in this RNA-processing mechanism [1].

Owing to its interaction with RNA-processing proteins and its localization within the SGs, we had previously proposed a role for DNMT2 in RNA processing during environmental stress to the cell. In the present study, we show that DNMT2 not only associates but also methylates different species of mRNA. Previous reports have suggested DNMT2 to be a tRNA methyltransferase, methylating a specific cytosine present within the CpG dinucleotide context in the tRNA [14–16]. In addition to methylating tRNA, the previous report also showed methylation of a specific cytosine, confined within a tRNA-type stem-loop structure, in the KRT18 mRNA by DNMT2 [41]. However, we find that DNMT2 can bind to and methylate different mRNA species including RPL27A, BRWD1 and CNNM3. RPL27A, a ribosomal protein, is a constituent of the 60S ribosomal subunit; CNNM3, a transmembrane protein, is a metal transporter and BRWD1 is associated with transcription activation and chromatin remodelling. All these proteins are important in different cellular pathways, but in response to stress their untranslated transcripts co-localize with DNMT2 in the cytoplasm, which is known to be localized to SGs. Neither did we find any sequence similarity or consensus motif between these different

mRNA species nor was methylation limited to cytosines present within CpG dinucleotides. Moreover, none of the cytosines that were found to be methylated in RPL27A were present in a tRNA-type stem-loop structure. Binding studies showed that DNMT2 could bind mRNA in a sequence-independent manner and preferred RNA as a substrate over DNA. Even RNA corresponding to the pBSK vector was found to bind to DNMT2. Therefore, the cytosine methylation activity of DNMT2 was similar to the other known eukaryotic cytosine methyltransferases that can methylate cytosines in a sequence-independent manner. However, it would be important to test a larger cohort of mRNA species that localize to the SGs to find out whether any signature sequence or structure motifs determine the mRNA methylation specificity of DNMT2.

HIV-1 uses DNMT2 to increase viral load in the host cell

Upon HIV-1 infection, DNMT2 was found to be re-localized from the nucleus to the cytoplasmic SGs (**Figure 1A**). During infection, HIV exploits the host mRNA transcription machinery to transcribe and replicate itself [42]. Reports have also shown HIV-2 genomic RNA to be a part of SGs [35]. Since DNMT2 is part of the SGs, it was possible that re-localization of DNMT2 was coincidental to the assembling of RNA-processing machinery in the SGs. It was also possible that DNMT2 was being used by the cell as part of its defence mechanism against the virus. Therefore, it was a surprise to find that overexpression of DNMT2 leads to an increase in the HIV-1 viral titre. It was also interesting to find that, in conjunction with increased HIV-1 load, the stability of HIV-1 RNA also increased in the presence of DNMT2. This suggested that HIV-1 was, in fact, using DNMT2 and piggybacking on its role in RNA methylation and processing to multiply and establish its infection. This is in contrast with the previous finding that, in *Drosophila*, DNMT2 through its RNA methylation activity was part of its antiviral defence [43]. It would be interesting not only to find the reason for this contrasting function of an evolutionarily conserved protein, DNMT2, in two different species but also to examine whether any viral protein was involved in actively bringing DNMT2 to SGs, thereby allowing the virus to hijack the RNA-processing machinery of the host cell to its own advantage.

While cytosine methylation has been shown to stabilize tRNA secondary structures, the effect of cytosine methylation in mRNA molecules has not been elucidated [44]. Our finding that DNMT2 methylates HIV RNA and mRNA and provides it post-transcriptional stability would argue that methylation of mRNA species by DNMT2 stabilizes them possibly by preventing their decay. The decision to either process mRNA for decay or storage or process it for other fates in the SGs has remained largely enigmatic. Therefore, cytosine methylation by DNMT2 providing stability to mRNA provides an important clue to the process of decision-making in the SGs. The next step in uncovering the various steps of this decision-making would be to identify mRNA species that are methylated in the SGs and find if they have any sequence or structure motifs that make them a target for stabilization by DNMT2.

Localization of DNMT2 is dependent on its phosphorylation

Re-localization of proteins within different intracellular compartments is known to be regulated by various post-translational modifications including phosphorylation [31]. DNMT2 lacks any canonical nuclear localization and nuclear export signals, and the mechanism of its re-localization to cytoplasmic SGs in response to environmental stress has remained unknown. Therefore, the finding that the re-localization of DNMT2 to SGs in response to HIV infection or other environmental stress was dependent on ATM kinase-mediated phosphorylation provides an important clue to the mechanism and pathways by which DNMT2 functions. It was interesting to find that ATM kinase, a protein that has been found to be crucial for HIV DNA integration into the host DNA and HIV-1 replication, was phosphorylating DNMT2, a protein that provides stability to HIV-1 RNA [45]. This would indicate that HIV probably utilizes the function of multiple proteins to multiply and perpetuate itself.

SG genesis is essential for the cell to endure environmental stress [1]. We show in the present study that HIV-1 utilizes the RNA methylation activity of DNMT2, a protein that is part of this essential cellular mechanism, to overcome the host defence mechanism and improve its own survivability. DNMT2 is an evolutionarily conserved protein that acts against viral infection in one species, but is being utilized by a virus for its own benefit in another. A comparative study of the relationship of DNMT2 with viruses in *Drosophila* and mammals would not only be important to dissect out the mechanism of its action but also open up a novel frontier in the study of host-pathogen interaction.

Abbreviations

³H-SAM, tritiated S-adenosylmethionine; BRWD1, Bromodomain and WD repeat domain containing 1; BSA, bovine serum albumin; CNNM3, cyclin M3; DNMT2, DNA methyltransferase 2; DPM, disintegrations per minute; EMSA, electrophoretic mobility shift assay; ER, endoplasmic reticulum; MCS, multiple cloning site; MeRIP-RT-PCR, methylated RNA immunoprecipitation RT-PCR; RPL27A, ribosomal protein L27A; SFB, protein S-Flag-biotin; SFB-ATM_K, SFB-tagged ATM kinase domain; SG, stress granules; TCA, trichloroacetic acid; TRAF, TNF receptor associated factors.

Author Contribution

S.K. and R.R.D. designed the experiments. R.R.D. performed the experiments. Experimental work related to HIV was planned in consultation with S.B. and S.M. and performed by R.R.D. with help from R.G. and S.P.S. in the laboratory of S.B. and S.M., respectively. S.K. and R.R.D. wrote the manuscript.

Funding

The present study was supported by funds from the Centre for DNA Fingerprinting and Diagnostics.

Acknowledgements

R.R.D. and R.G. are recipients of Senior Research Fellowship of the Council of Scientific and Industrial Research (CSIR), India towards the pursuit of a PhD degree of the Manipal University, Manipal and University of Hyderabad, Hyderabad, respectively.

Competing Interests

The Authors declare that there are no competing interests associated with the manuscript.

References

- 1 Kedersha, N., Stoecklin, G., Ayodele, M., Yacono, P., Lykke-Andersen, J., Fitzler, M.J. et al. (2005) Stress granules and processing bodies are dynamically linked sites of mRNP remodeling. *J. Cell Biol.* **169**, 871–884 doi:10.1083/jcb.200502088
- 2 Anderson, P. and Kedersha, N. (2008) Stress granules: the Tao of RNA triage. *Trends Biochem. Sci.* **33**, 141–150 doi:10.1016/j.tibs.2007.12.003
- 3 Kedersha, N. and Anderson, P. (2009) Chapter 4 Regulation of translation by stress granules and processing bodies. *Prog. Mol. Biol. Transl. Sci.* **90**, 155–185 doi:10.1016/S1877-1173(09)90004-7
- 4 Kedersha, N.L., Gupta, M., Li, W., Miller, I. and Anderson, P. (1999) RNA-binding proteins Tia-1 and Tiar link the phosphorylation of Eif-2 α to the assembly of mammalian stress granules. *J. Cell Biol.* **147**, 1431–1442 doi:10.1083/jcb.147.7.1431
- 5 Anderson, P. and Kedersha, N. (2002) Visibly stressed: the role of eIF2, TIA-1, and stress granules in protein translation. *Cell Stress Chaperones* **7**, 213–221 doi:10.1379/1466-1268(2002)007<0213:VSTROE>2.0.CO;2
- 6 Kimball, S.R., Horetsky, R.L., Ron, D., Jefferson, L.S. and Harding, H.P. (2003) Mammalian stress granules represent sites of accumulation of stalled translation initiation complexes. *Am. J. Physiol. Cell Physiol.* **284**, C273–C284 doi:10.1152/ajpcell.00314.2002
- 7 Tourrière, H., Cheblí, K., Zekri, L., Courselaud, B., Blanchard, J.M., Bertrand, E. et al. (2003) The RasGAP-associated endoribonuclease G3BP assembles stress granules. *J. Cell Biol.* **160**, 823–831 doi:10.1083/jcb.200212128
- 8 Gilks, N., Kedersha, N., Ayodele, M., Shen, L., Stoecklin, G., Dember, L.M. et al. (2004) Stress granule assembly is mediated by prion-like aggregation of TIA-1. *Mol. Biol. Cell* **15**, 5383–5398 doi:10.1091/mbc.E04-08-0715
- 9 Tsai, N.P., Ho, P.-C. and Wei, L.-N. (2008) Regulation of stress granule dynamics by Grb7 and FAK signalling pathway. *EMBO J.* **27**, 715–726 doi:10.1038/emboj.2008.19
- 10 Kwon, S., Zhang, Y. and Matthias, P. (2007) The deacetylase HDAC6 is a novel critical component of stress granules involved in the stress response. *Genes Dev.* **21**, 3381–3394 doi:10.1101/gad.461107
- 11 Thiagarajan, D., Dev, R.R. and Khosla, S. (2011) The DNA methyltransferase Dnmt2 participates in RNA processing during cellular stress. *Epigenetics* **6**, 103–113 doi:10.4161/epi.6.1.13418
- 12 Weeks, A., Agnihotri, S., Lymer, J., Chalil, A., Diaz, R., Isik, S. et al. (2016) Epithelial cell transforming 2 and Aurora kinase B modulate formation of stress granule-containing transcripts from diverse cellular pathways in astrocytoma cells. *Am. J. Path.* **186**, 1674–1687 doi:10.1016/j.ajpath.2016.02.013
- 13 Kim, W.J., Back, S.H., Kim, V., Ryu, I. and Jang, S.K. (2005) Sequestration of TRAF2 into stress granules interrupts tumor necrosis factor signaling under stress conditions. *Mol. Cell. Biol.* **25**, 2450–2462 doi:10.1128/MCB.25.6.2450-2462.2005
- 14 Goll, M.G., Kirpekar, F., Maggert, K.A., Yoder, J.A., Hsieh, C.-L., Zhang, X. et al. (2006) Methylation of tRNAAsp by the DNA methyltransferase homolog Dnmt2. *Science* **311**, 395–398 doi:10.1126/science.1120976
- 15 Schaefer, M., Pollex, T., Hanna, K., Tuorto, F., Meusburger, M., Helm, M. et al. (2010) RNA methylation by Dnmt2 protects transfer RNAs against stress-induced cleavage. *Genes Dev.* **24**, 1590–1595 doi:10.1101/gad.586710
- 16 Tuorto, F., Liebers, R., Musch, T., Schaefer, M., Hofmann, S., Kellner, S. et al. (2012) RNA cytosine methylation by Dnmt2 and NSun2 promotes tRNA stability and protein synthesis. *Nat. Struct. Mol. Biol.* **19**, 900–905 doi:10.1038/nsmb.2357
- 17 Jurkowski, T.P., Meusburger, M., Phalke, S., Helm, M., Nellen, W., Reuter, G. et al. (2008) Human DNMT2 methylates tRNA Asp molecules using a DNA methyltransferase-like catalytic mechanism. *RNA* **14**, 1663–1670 doi:10.1261/rna.970408

- 18 Rai, K., Chidester, S., Zavala, C.V., Manos, E.J., James, S.R., Karpf, A.R. et al. (2007) Dnmt2 functions in the cytoplasm to promote liver, brain, and retina development in zebrafish. *Genes Dev.* **21**, 261–266 doi:10.1101/gad.1472907
- 19 Durdevic, Z., Mobin, M.B., Hanna, K., Lyko, F. and Schaefer, M. (2013) The RNA methyltransferase dnmt2 is required for efficient dicer-2-dependent siRNA pathway activity in *Drosophila*. *Cell Rep.* **4**, 931–937 doi:10.1016/j.celrep.2013.07.046
- 20 Lin, M.-J., Tang, L.-Y., Reddy, M.N. and Shen, C.-K.J. (2005) DNA methyltransferase gene dDnmt2 and longevity of *Drosophila*. *J. Biol. Chem.* **280**, 861–864 doi:10.1074/jbc.C400477200
- 21 Phalke, S., Nickel, O., Walluscheck, D., Hörtig, F., Onorati, M.C. and Reuter, G. (2009) Retrotransposon silencing and telomere integrity in somatic cells of *Drosophila* depends on the cytosine-5 methyltransferase DNMT2. *Nat. Gen.* **41**, 696–702 doi:10.1038/ng.360
- 22 Tuorto, F., Herbst, F., Alerasool, N., Bender, S., Popp, O., Federico, G. et al. (2015) The tRNA methyltransferase Dnmt2 is required for accurate polypeptide synthesis during haematopoiesis. *EMBO J.* **34**, 2350–2362 doi:10.15252/embj.2015191382
- 23 Kiani, J., Grandjean, V., Liebers, R., Tuorto, F., Ghanbarian, H., Lyko, F. et al. (2013) RNA-mediated epigenetic heredity requires the cytosine methyltransferase Dnmt2. *PLoS Genet.* **9**, e1003498 doi:10.1371/journal.pgen.1003498
- 24 Arya, D., Kapoor, S. and Kapoor, M. (2016) Physcomitrella patens DNA methyltransferase 2 is required for recovery from salt and osmotic stress. *FEBS J.* **283**, 556–570 doi:10.1111/febs.13611
- 25 Sambrook, J. and Russell, D.W. (2001) *Molecular Cloning: A Laboratory Manual*, Cold Spring Harbor Laboratory Press, Cold Spring Harbor, NY
- 26 Kuthner, R.H., Zhang, X.-Y. and Reiser, J. (2009) Production, concentration and titration of pseudotyped HIV-1-based lentiviral vectors. *Nat. Protoc.* **4**, 495–505 doi:10.1038/nprot.2009.22
- 27 Xu, A., Jao, D.L.-E. and Chen, K.Y. (2004) Identification of mRNA that binds to eukaryotic initiation factor 5A by affinity co-purification and differential display. *Biochem. J.* **384**, 585–590 doi:10.1042/BJ20041232
- 28 Lewis, S.E. and Konradi, C. (1996) Analysis of DNA–protein interactions in the nervous system using the electrophoretic mobility shift assay. *Methods* **10**, 301–311 doi:10.1006/meth.1996.0107
- 29 Zurla, C., Lifland, A.W. and Santangelo, P.J. (2011) Characterizing mRNA interactions with RNA granules during translation initiation inhibition. *PLoS ONE* **6**, e19727 doi:10.1371/journal.pone.0019727
- 30 Beausoleil, S.A., Villén, J., Gerber, S.A., Rush, J. and Gygi, S.P. (2006) A probability-based approach for high-throughput protein phosphorylation analysis and site localization. *Nat. Biotechnol.* **24**, 1285–1292 doi:10.1038/nbt1240
- 31 Tourriere, H., Gallouzi, I.-e., Chebli, K., Capony, J.P., Mouaike, J., van der Geer, P. et al. (2001) RasGAP-associated endoribonuclease G3BP: selective RNA degradation and phosphorylation-dependent localization. *Mol. Cell. Biol.* **21**, 7747–7760 doi:10.1128/MCB.21.22.7747-7760.2001
- 32 Amanchy, R., Periaswamy, B., Mathivanan, S., Reddy, R., Tattikota, S.G. and Pandey, A. (2007) A curated compendium of phosphorylation motifs. *Nat. Biotechnol.* **25**, 285–286 doi:10.1038/nbt0307-285
- 33 Dong, A., Yoder, J.A., Zhang, X., Zhou, L., Bestor, T.H. and Cheng, X. (2001) Structure of human DNMT2, an enigmatic DNA methyltransferase homolog that displays denaturant-resistant binding to DNA. *Nucleic Acids Res.* **29**, 439–448 doi:10.1093/nar/29.2.439
- 34 Gilmartin, G.M., Fleming, E.S., Oetjen, J. and Graveley, B.R. (1995) CPSF recognition of an HIV-1 mRNA 3'-processing enhancer: Multiple sequence contacts involved in poly(A) site definition. *Genes Dev.* **9**, 72–83 doi:10.1101/gad.9.1.72
- 35 Soto-Rifo, R., Valiente-Echeverría, F., Rubilar, P.S., García-de-Gracia, F., Ricci, E.P., Limousin, T. et al. (2014) HIV-2 genomic RNA accumulates in stress granules in the absence of active translation. *Nucleic Acids Res.* **42**, 12861–12875 doi:10.1093/nar/gku1017
- 36 Khoddami, V. and Cairns, B.R. (2014) Transcriptome-wide target profiling of RNA cytosine methyltransferases using the mechanism-based enrichment procedure Aza-IP. *Nat. Protoc.* **9**, 337–361 doi:10.1038/nprot.2014.014
- 37 Jurkowski, T.P. and Jeltsch, A. (2011) On the evolutionary origin of eukaryotic DNA methyltransferases and Dnmt2. *PLoS ONE* **6**, e28104 doi:10.1371/journal.pone.0028104
- 38 Gokhale, N.S., McIntyre, A.B.R., McFadden, M.J., Roder, A.E., Kennedy, E.M., Gandara, J.A. et al. (2016) N⁶-methyladenosine in flaviviridae viral RNA genomes regulates infection. *Cell Host Microbe* **20**, 654–665 doi:10.1016/j.chom.2016.09.015
- 39 Lichinchi, G., Gao, S., Saleto, Y., Gonzalez, G.M., Bansal, V., Wang, Y. et al. (2016) Dynamics of the human and viral m⁶A RNA methylomes during HIV-1 infection of T cells. *Nat. Microbiol.* **1**, 16011 doi:10.1038/nmicrobiol.2016.11
- 40 Tirumuru, N., Zhao, B.S., Lu, W., Lu, Z., He, C. and Wu, L. (2016) N⁶-methyladenosine of HIV-1 RNA regulates viral infection and HIV-1 Gag protein expression. *eLife* **5**, e15528 doi:10.7554/eLife.15528
- 41 Khoddami, V. and Cairns, B.R. (2013) Identification of direct targets and modified bases of RNA cytosine methyltransferases. *Nat. Biotechnol.* **31**, 458–464 doi:10.1038/nbt.2566
- 42 Purcell, D.F. and Martin, M.A. (1993) Alternative splicing of human immunodeficiency virus type 1 mRNA modulates viral protein expression, replication, and infectivity. *J. Virol.* **67**, 6365–6378 PMID:8411338
- 43 Durdevic, Z., Hanna, K., Gold, B., Pollex, T., Cherry, S., Lyko, F. et al. (2013) Efficient RNA virus control in *Drosophila* requires the RNA methyltransferase Dnmt2. *EMBO Rep.* **14**, 269–275 doi:10.1038/embor.2013.3
- 44 Motorin, Y. and Helm, M. (2010) tRNA stabilization by modified nucleotides. *Biochemistry* **49**, 4934–4944 doi:10.1021/bi100408z
- 45 Lau, A., Swinbank, K.M., Ahmed, P.S., Taylor, D.L., Jackson, S.P., Smith, G.C.M. et al. (2005) Suppression of HIV-1 infection by a small molecule inhibitor of the ATM kinase. *Nat. Cell Biol.* **7**, 493–500 doi:10.1038/ncb1250